ARMA 22–360

Application of a coupled thermo-hydro-mechanical-chemical simulation to a North Sea hydrocarbon chalk reservoir

Hosseinzadehsadati, S.B., Amour, F., Hajiabadi, M.R., Nick. H.M.

DTU offshore, Technical University of Denmark, Kgs. Lyngby, Denmark

ABSTRACT: Water weakening effect in the chalk reservoir causes additional compaction due to the interaction between the rock and injected water. To consider the impact of the coupled interactions on the fluid transport (e.g., production) and reservoir deformation due to the seawater injection into the chalk reservoirs, in this study, a wrapper is developed in Matlab that combines Eclipse 100 reservoir simulator and Visage geomechanics simulator to capture the induced alteration of mechanical and petrophysical properties of chalk. Here, we utilize the history-matched reservoir model of the Halfdan sector model to investigate the impact of the temperature-dependent fluid-rock interactions induced by sulfate adsorption on the surface of calcite grains on the deformation behavior of the reservoir during waterflooding. Our sector-scale simulation results show that while considering the geomechanics model has a considerable impact on calculated reservoir pressure and recovery, the impact on history matched data due to water weakening is not significant when yield stress and bulk modulus are expressed as functions of temperature and sulfate concentration for the Halfdan model. We argue that the minor contribution of the water weakening effect at *in situ* conditions is due to 1) the relatively high initial water saturation in the water flooded section of the reservoir and 2) the low initial temperature (70 ˚C) of Halfdan reservoir, especially towards the northern part of the Danish North Sea.

1. INTRODUCTION

High porosity and low permeability chalk reservoirs respond significantly to the interaction of Thermal, Hydrological, Mechanical, and Chemical (THMC) effects that causes changes in rock porosity and permeability that ultimately influence the performance of hydrocarbon production (Minde & Hiorth, 2019). Generally, as the reservoir pressure is reduced during production, the effective stress increases, causing the reservoir to compact, a mechanism that can potentially enhance production (Barkved et al., 2003). However, not only does pore pressure reduction causes subsurface deformation and subsequently seabed subsidence, but water injection may also lead to additional compaction in the North Sea fields (Doornhof et al., 2006). For example, cold seawater has been injected to improve oil recovery in the North Sea hydrocarbon chalk fields for many years. This has caused a softening of the rock strength (i.e., yield stress) and stiffness (i.e., bulk modulus), referred to as the water weakening effect. Megawati et al. (2013) and Røyne et al. (2015) that rock softening results from the adsorption of water molecules and key ions such as magnesium and sulfate from the aqueous phase to the surface of calcite grains. The water weakening effect is also dependent on the temperature. Both an increase in temperature and sulfate concentration favor a high repulsive force between calcite grains, thereby a more pronounced weakening of chalk strength and stiffness. Besides, the amount of ion adsorbed on the chalk surface is dependent on pH, salinity, surface properties, and the presence of other ions. Therefore, the injection of seawater with different chemical compositions and temperatures compared to those of the reservoir fluid can significantly impact the behavior of the reservoir intricately.

It is crucial to accurately estimate the rate- and fluid-dependent evolution of elasto-plastic strain in chalk to minimize the risk associated with subsurface deformation and sea-floor subsidence. However, for the field scale simulations of water-induced compaction in chalk, using only water saturation as an indicator of compaction may introduce error to the simulated system for history matching of production data. Therefore, the model is needed to couple the interactions of fluid transport and reservoir compaction to provide a reliable and more applicable tool for forecasting reservoir deformation and production. In this study, we address the water weakening effect in a Danish North Sea reservoir by considering the temperature-dependent softening of the rock strength and stiffness caused by the adsorption of sulfate ions from the aqueous phase to the surface of calcite grains.

2. HALFDAN FIELD

The Halfdan field is located in the southern part of the Danish North Sea, close to the Dan field. The hydrocarbon accumulation is controlled by a combination of stratigraphic and dynamic traps (Albrechtsen et al., 2001). The main Halfdan field is an oil reservoir situated in the Upper Tor formation, where the porosity ranges from 20% to 35% and associated permeability of 1 to 5 mD. The initial pore pressure was estimated at around 29 MPa (Amour et al., 2021). The field was discovered in late 1998 at depth of 2100 m and began producing at the end of 1999. The Halfdan field is developed with long, parallel sub-horizontal alternating production and injection wells with a distance of 190 m (Calvert et al., 2016). The primary reservoir-drive mechanism of the Halfdan field is waterflooding. However, a well generally produces oil for up to six months before being converted to a water injection well. In this study, a sector model (Fig. 1) with three production and four injection wells is used to capture the impact of the induced alteration of mechanical and petrophysical properties of chalk by waterflooding and its effect on oil production and reservoir pressure.

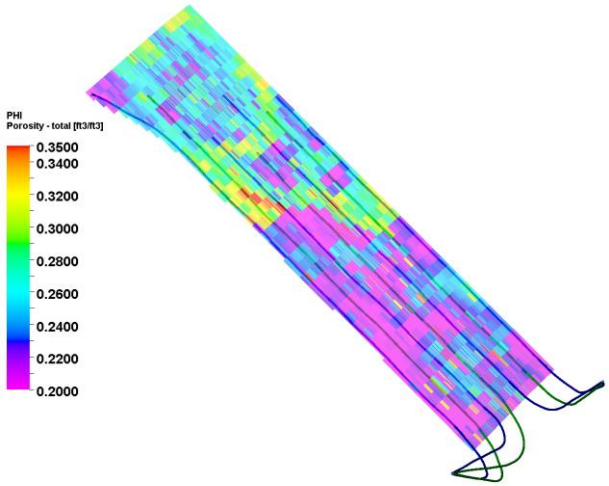

Fig. 1. Map view of porosity distribution for the selected sector model contains four injection and three production wells with an average well spacing of 190 m. The 3D sector model has a size of 440×5264×860 m^3 and is discretized into 78×45×88 grid blocks for the flow simulations (Taheriotaghsara et al., 2020). The same asks the real case, parallel hydraulic fractures are implemented in the model to increase well sweep efficiency and injectivity. The three wells in the middle contain finer mesh size compared with other parts of the sector model. Therefore, in this study, we mainly report the production data of the middle well.

3. METHODOLOGY

Observing the compaction of a hydrocarbon reservoir is difficult; however, measuring subsidence at the surface is not often challenging. For offshore fields, however, subsidence is monitored at platforms. To this end, for the Halfdan field, seafloor subsidence is measured by three GPS surveys carried out on a platform and covering an approximately ten years production period. The error associated with the measurements is less than 5 cm compaction (Amour et al., 2021).

3.1. Geomechanical model configuration

A 3D geomechanical model (Fig. 2) is built to evaluate how sulfate ions in the seawater modify the constitutive properties of the chalk and mechanically weaken it as well as the reservoir compaction due to pressure drawdown. According to a total of 593 RFT data collected from the Halfdan field (Amour et al., 2021), the pore pressure of 13500 Pa/m and 8930 Pa/m are used along the overburden and within the reservoir, respectively. It is assumed that the overburden and underburden are shale-dominated (Bonto et al., 2021) while sideburden and reservoir are chalk-dominated.

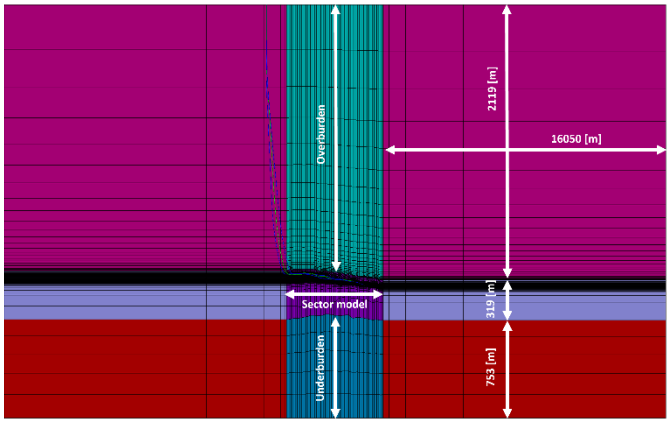

Fig. 2. Schematic of the geomechanical model in a vertical plane. 5 number of grid blocks are assigned for both x- and y-direction, and 25 and 5 for overburden and underburden, respectively. In total the geomechanical model consists of 586340 grid-blocks. Z scale or vertical exaggeration of 5 is set to clarify the thickness of the sector model.

3.2. Fluid and rock properties

Eclipse 100 is used to solve non-isothermal multiphase flow and multicomponent transport. Ion adsorption on the rock surface as a function of ionic concentration is implemented by employing the environmental tracer option in Eclipse 100 (Fig. 3). Taheriotaghsara et al. (2020) estimate the amount of sulfate adsorption on the calcite surface by using PHREEQC and setting a specific surface area (SSA) of 2.5 m^2/g. The amount of active surface site density equal to 4.95 $\#/nm^2$. The sulfate concentration for Halfdan formation water and seawater is assumed to be similar to 0.069 and 2.707 kg/m^3, respectively (Schovsbo et al., 2018). Halfdan reservoir temperature is considered to be 70 ˚C and constant all over the reservoir. The surface temperature of seawater is approximately 7 ˚C in winter and between 15-19 ˚C in summer (Maersk Oil, 2015); however, we assume that the bottomhole seawater temperature is 30 ˚C when injecting into the reservoir.

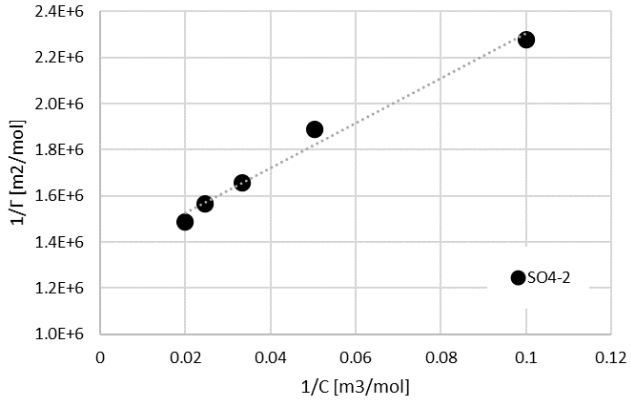

Fig. 3. Amount of SO_4^{-2} ion adsorbed (Γ_i) versus its concentration in the aqueous phase (C_i)

This study uses a Visage finite element simulator to predict subsidence, compaction, and pore collapse due to high-pressure draw-down during production operations. We take into account the dependency of mechanical behavior of Danian and Maastrichtian chalk to porosity, strain hardening, water saturation and strain rate by calibrating in situ compaction measurements and experimental data (Amour et al., 2021; Amour et al., 2021). Table 1. and Table 2 summarize the porosity-dependent input functions for the reservoir and the porosity-independent parameters for overburden. The Biot coefficient and Poisson's ratio are assumed equal to 1 and 0.2 during calculation.

Table 1. Summarized input functions of the porosity-dependent geomechanical parameters. E = Young's modulus, ϕ = porosity, P_t = tensile strength, φ = angle of internal friction, P_c = initial hydrostatic pore collapse strength, e = initial void ratio, χ = hardening coefficient, λ and κ are the two compression coefficients, h = hardening parameter, and C'= cohesion

$E\ [MPa]$	$83140e^{(-8.49\phi)}$
$P_t[MPa]$	$4.8 - 6.4\phi$
$\varphi[rad]$	$1.09e^{(-1.6\phi)}$
$P_c[MPa]$	$1180e^{(-10.3\phi)}$
e	$\phi/(1-\phi)$
χ	$(\lambda-\kappa)/(1+e)$
$h\ [MPa]$	P_c/χ
$C'[MPa]$	$13.2e^{(-5.4\phi)}$

Table 2. Summarized porosity-independent geomechanical parameters for overburden, underburden and sideburden

Parameters	Overburden	Underburden	Sideburden
$E\ [MPa]$	36000.00	36000.00	15237.41
$P_t[MPa]$	6.00	6.00	3.52
$\varphi[rad]$	0.25	0.25	0.79
$P_c[MPa]$	-	-	327
$h\ [MPa]$	-	-	1571.52
$C'[MPa]$	-	-	3.56

Fig. 4 shows the hydrostatic pore collapse strength and bulk modulus as a function of temperature and sulfate concentration based on the literature data (Korsnes et al., 2008; Madland et al., 2011; Megawati et al., 2013). During simulation, these aforementioned material parameters are updated in the simulation for the next geomechanical time step based on temperature and sulfate concentration front calculated by Eclipse 100.

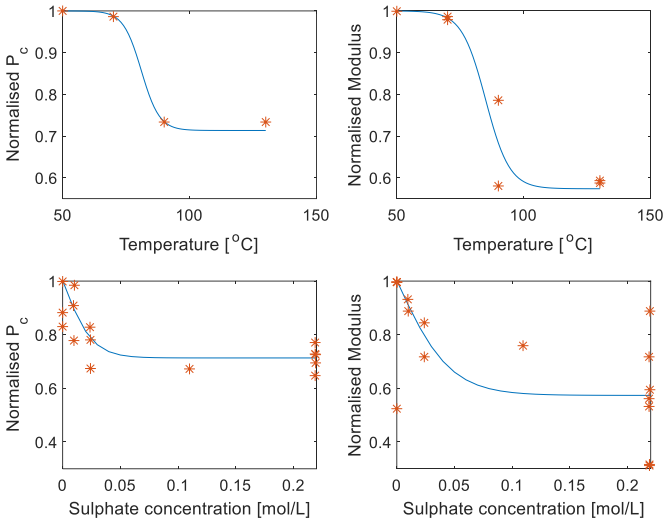

Fig. 4. Relationships between temperature and sulfate concentration, and yield stress and bulk modulus (star marker: experiment data, solid blue line: correlation)

3.3. Numerical examples

Three coupled simulation cases are run and compared with the initial history matched model in order to estimate the importance of considering coupled processes in assessing seafloor subsidence, injectivity and hydrocarbon production. Note that the initial history matched model does not consider deformation and only solves for multiphase flow in the reservoir. The three cases are:

- Model 1: permeability and porosity are updated dynamically in Eclipse 100 by using results from the geomechanical model obtained from Visage
- Model 2: permeability and porosity are updated dynamically in Eclipse 100 by using results from the geomechanical model obtained from Visage when the water weakening effect is active in Visage
- Model 3: permeability and porosity are updated dynamically in Eclipse 100, where yield stress and bulk modulus are both temperature- and sulfate-dependent and change during the geomechanical simulation time step while the water weakening effect is active in Visage

Porosity is updated from the volumetric strain occurring as a result of the pore pressure change between the two stress steps:

$$\phi = \phi_0 + \alpha\Delta\varepsilon_v$$

where α is Biot's coefficient and $\Delta\varepsilon_v$ is change in volume strain. According to the Kozeny-Carman equation (Carman, 1997), the permeability is updated based on the initial permeability and porosity, as well as the updated porosity as follows:

$$K = K_0 \frac{\phi^3/(1-\phi)^2}{\phi_0^3/(1-\phi_0)^2}$$

It is important to mention that the permeability and porosity are updated in the reservoir simulator repeatedly until a given tolerance (1×10^{-4}) is achieved.

4. RESULTS

4.1. History-matched data

A better understanding of chalk failure leads to improve production methods since the rock drive can be many times greater than the fluid-expansion drive for the North Sea chalks. Fig. 5 illustrates the impact of volume strain change on porosity/permeability, leading to the pressure difference. In the case of history-matching the bottom-hole pressure data, this effect cannot be underestimated, as shown in Fig. 6.

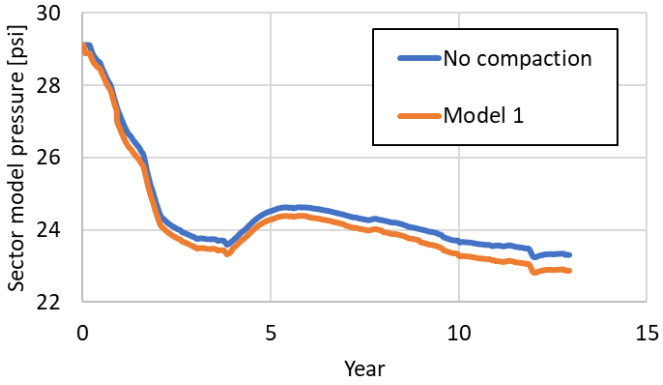

Fig. 5. The sector model pressure in the present (orange line) and absent (blue line) of porosity/permeability change caused by geomechanical impacts

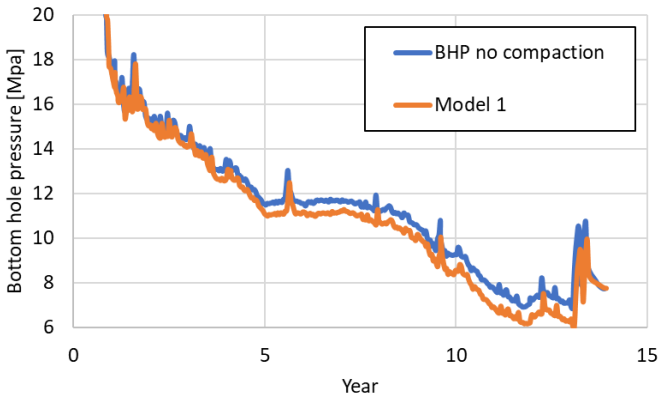

Fig. 6. Comparison of the bottom-hole pressure of the middle well of the sector model in the present (orange line) and absent (blue line) of porosity/permeability change caused by geomechanical impacts

4.2. Water weakening effect

Average water saturation in Tor formation in Halfdan reservoir is above 25%. As described in technical description of Visage, most of the pore collapse strength decrease takes place while the water saturation of chalk increases to about 25%. Fig. 7 shows the pore collapse strength sensitivity as a function of water saturation. This means that an increase of water saturation by seawater injection into Halfdan reservoir has a less impact on pore collapse strength (Fig. 8). However, Fig. 8 shows that using yield stress and bulk modulus as a function of temperature and sulfate concentration has also limited impact on the sector model pressure since mostly effects on geomechanics takes place at temperature higher than 90 ˚C and higher sulfate concentration (Fig. 4). It is worth mentioning that in this study we assume that the water saturation has no impact on hardening effect.

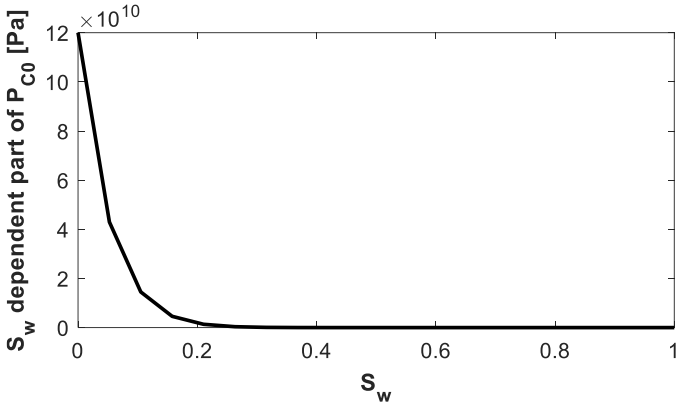

Fig. 7. Impact of water saturation on hydrostatic pore collapse strength change compared with the initial value of P_{C0}

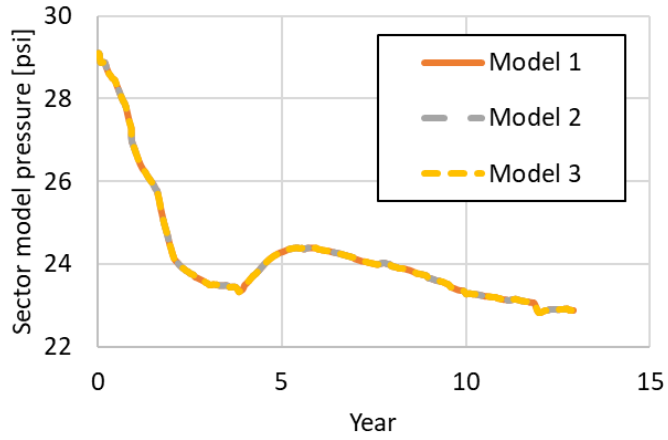

Fig. 8. Comparison of the sector model pressure between Model 1, 2, and 3

4.3. Reservoir compaction

The vertical displacement simulations at the top of the reservoir and seafloor for the three models are investigated. Fig. 9 shows that the top reservoir displacement is the same for three models. This means that neither water weakening option included in Visage nor yield stress plus bulk modulus temperature- and sulfate-dependent has insignificant impact on the displacement because of initial high water saturation and low temperature of Halfdan chalk reservoir. The rate of sea-floor subsidence measured by GPS is compared with

simulation results in Fig. 10, where the simulation underestimate vertical displacement by a factor of 30% (still within the accuracy range of measured GPS data). A poor prediction of sea-floor subsidence can be explained by using an inappropriate simulation input data or not updating the well connections during the simulation. By comparing the vertical strain at the top of Tor formation, Fig. 11 illustrates that reservoir does not compact a lot over time.

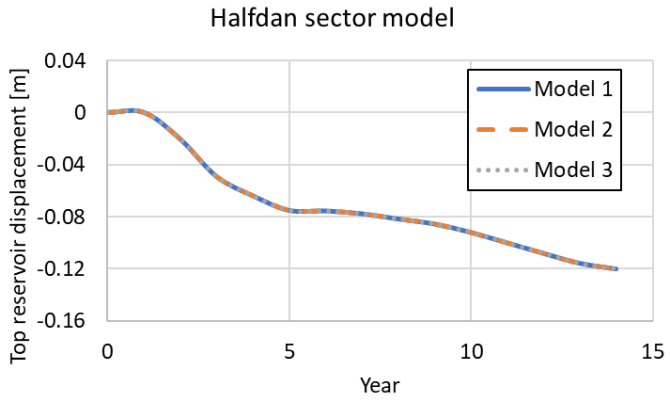

Fig. 9. Comparison of simulation results of top reservoir displacement from three different models for Halfdan sector model

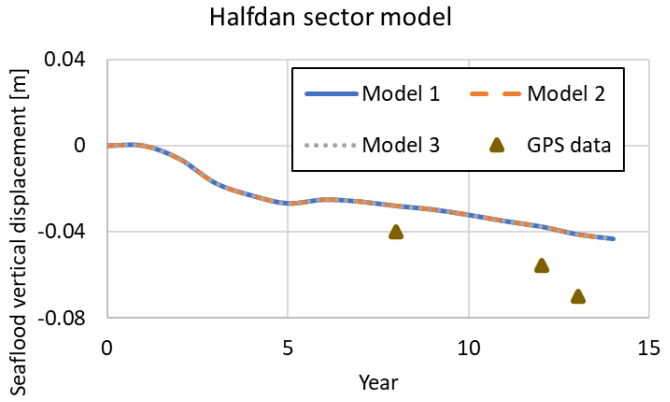

Fig. 10. Comparison of simulation results from three different models and observed sea-floor vertical subsidence data of oil production and seawater injection for Halfdan sector model

(a)

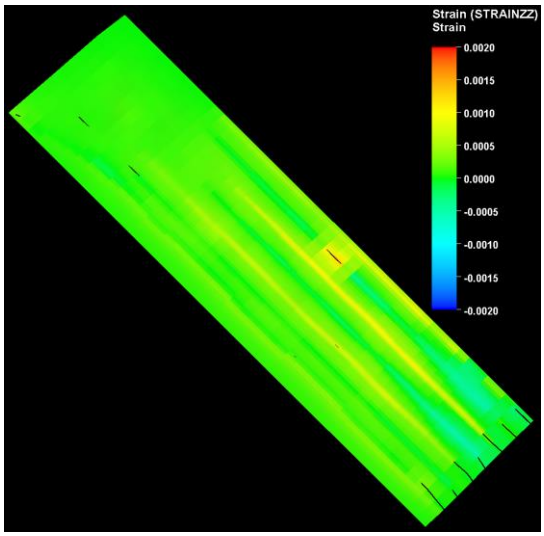

(b)

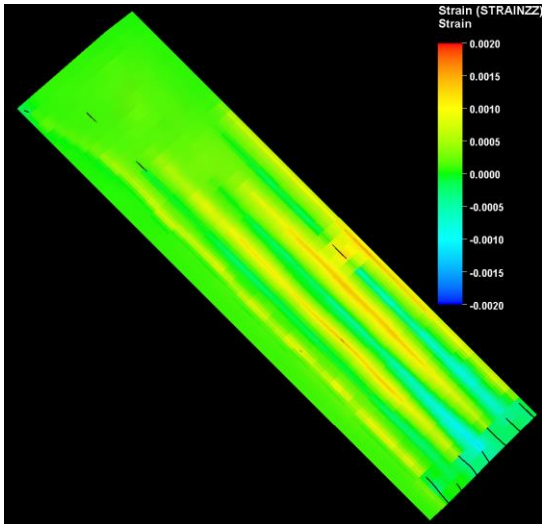

Fig. 11. Evolution of vertical strain at the top of Tor formation at a) 2005 b) 2015

5. CONCLUSION

This study is an initial step towards the modeling of the rock - fluid interaction impacts on compaction at the field scale for the Danish North Sea hydrocarbon chalk reservoirs. For this purpose, a wrapper is developed in Matlab that combines Eclipse reservoir simulator and Visage geomechanics simulator to capture the rock - fluid interaction impacts on mechanical and petrophysical properties of Halfdan chalk reservoir. The developed model utilizes the output of Eclipse 100 simulation results and employ the yield stress correlations as a function of temperature and sulfate concentration to update the mechanical properties of each grid block. Then, the porosity and permeability values are updated for the next time step, based on the Visage's output.

Three geomechanical scenarios are considered to estimate the mechanical impacts on the ultimate reservoir pressure, porosity and permeability change. Comparison of history matched data reveals that the production well pressure is influenced more than the injection wells due to the high pressure drop. Also, the simulation results from Model 2 indicates that activating the water weakening option has an insignificant influence on mechanical and petrophysical properties of chalk due to the fact that the initial water saturation of Halfdan chalk reservoir is more high in the water-swept zones of the reservoir. Moreover, updating yield stress and bulk modulus based on temperature and sulfate concentration result in trivial impact on the ultimate recovery factor and bottom-hole pressure calculated for the Halfdan field since the effects on geomechanics mostly takes place at temperature higher than 90 ˚C and higher sulfate concentration more than that of 0.028 mol/L.

Considering the low deformation that Halfdan field has experienced this comparative study needs to be evaluated for the fields with higher compaction and lower initial water saturation.

REFERENCES

Albrechtsen, T., Andersen, S. J., Dons, T., Engstrøm, F., Jørgensen, O., & Sørensen, F. W. (2001). Halfdan: Developing Non-Structurally Trapped Oil in North Sea Chalk. *Proceedings - SPE Annual Technical Conference and Exhibition*, 75–88. https://doi.org/10.2118/71322-MS

Amour, F., Christensen, H. F., Hajiabadi, M. R., & Nick, H. M. (2021). Effects of Porosity and Water Saturation on the Yield Surface of Upper Cretaceous Reservoir Chalks From the Danish North Sea. *Journal of Geophysical Research: Solid Earth*, *126*(3), e2020JB020608. https://doi.org/10.1029/2020JB020608

Amour, F., Hajiabadi, M. R., & Nick, H. M. (2021). Building a comprehensive geomechanical model for chalk compaction. Phase 2: 1-D simulation of two Danish reservoirs. *55th U.S. Rock Mechanics / Geomechanics Symposium 2021*, *5*.

Barkved, O., Heavey, P., Kjelstadli, R., Kleppan, T., & Kristiansen, T. G. (2003). Valhall Field - Still on Plateau after 20 Years of Production. *Society of Petroleum Engineers - SPE Offshore Europe Oil and Gas Exhibition and Conference 2003, OE 2003*. https://doi.org/10.2118/83957-MS

Bonto, M., Welch, M. J., Lüthje, M., Andersen, S. I., Veshareh, M. J., Amour, F., Afrough, A., Mokhtari, R., Hajiabadi, M. R., Alizadeh, M. R., Larsen, C. N., & Nick, H. M. (2021). Challenges and enablers for large-scale CO2 storage in chalk formations. *Earth-Science Reviews*, *222*, 103826. https://doi.org/10.1016/j.earscirev.2021.103826

Calvert, M. A., Hoover, A. R., Vagg, L. D., Ooi, K. C., & Hirsch, K. K. (2016). Halfdan 4D workflow and results leading to increased recovery. *The Leading Edge*, *35*(10), 840–848. https://doi.org/10.1190/tle35100840.1

Carman, P. G. (1997). Fluid flow through granular beds. *Chemical Engineering Research and Design*, *75*(1 SUPPL.), S32–S48. https://doi.org/10.1016/S0263-8762(97)80003-2

Doornhof, D., Kristiansen, T. G., Nagel, N. B., Pattillo, P. D., & Sayers, C. (2006). Compaction and subsidence. In *Oilfield Review* (Vol. 18, Issue 3, pp. 50–68). http://www-geology.ucdavis.edu/~cowen/~GEL115/

Korsnes, R. I., Madland, M. V., Vorland, K. A. N., Hildebrand-Habel, T., Kristiansen, T. G., & Hiorth, A. (2008). *2008: Enhanced Chemical Weakening of Chalk Due to Injection of Co2 Enriched Water, in: Society of Core Analysts. Presented at the International Symposium of the Society of Core Analysts, Abu Dhabi, UAE*. 12. https://www.scopus.com/inward/record.uri?eid=2-s2.0-85117081269&partnerID=40&md5=f77536d0daac5d3b71acf85c765cb773

Madland, M. V., Hiorth, A., Omdal, E., Megawati, M., Hildebrand-Habel, T., Korsnes, R. I., Evje, S., & Cathles, L. M. (2011). Chemical Alterations Induced by Rock–Fluid Interactions When Injecting Brines in High Porosity Chalks. *Transport in Porous Media 2011 87:3*, *87*(3), 679–702. https://doi.org/10.1007/S11242-010-9708-3

Maersk Oil. (2015). *MAERSK OIL ESIA-16 NON-TECHNICAL SUMMARY-ESIS HALFDAN Maersk Oil Non-Technical Summary (NTS)*. www.ens.dk.

Megawati, M., Hiorth, A., & Madland, M. V. (2013). The impact of surface charge on the mechanical behavior of high-porosity chalk. *Rock Mechanics and Rock Engineering*, *46*(5), 1073–1090. https://doi.org/10.1007/s00603-012-0317-z

Minde, M. W., & Hiorth, A. (2019). Compaction and Fluid—Rock Interaction in Chalk Insight from Modelling and Data at Pore-, Core-, and Field-Scale. *Geosciences 2020, Vol. 10, Page 6*, *10*(1), 6. https://doi.org/10.3390/GEOSCIENCES10010006

Røyne, A., Dalby, K. N., Hassenkam, T., Røyne, A., Dalby, K. N., & Hassenkam, T. (2015). Repulsive hydration forces between calcite surfaces and their effect on the brittle strength of calcite-bearing rocks. *GeoRL*, *42*(12), 4786–4794. https://doi.org/10.1002/2015GL064365

Schovsbo, N. H., Gottfredsen, S. N., Schmidt, K. G., & Jørgensen, T. M. (2018). Oil production monitoring and optimization from produced water analytics; a case study from the Halfdan chalk oil field, Danish North Sea. *IFAC-PapersOnLine*, *51*(8), 203–210. https://doi.org/10.1016/J.IFACOL.2018.06.378

Taheriotaghsara, M., Bonto, M., Eftekhari, A. A., & Nick, H. M. (2020). Prediction of oil breakthrough time in modified salinity water flooding in carbonate cores. *Fuel*, *274*(xxxx). https://doi.org/10.1016/j.fuel.2020.117806

Taheriotaghsara, M., Hosseinzadehsadati, S., & Nick, H. M. (2020). The Impact of Spatially Correlated Heterogeneity and Adsorption on Modified Salinity Water in Carbonates. *ACS Omega*, *5*(46), 29780–29794. https://doi.org/10.1021/acsomega.0c03679